COMPARISON OF DIMENSIONAL ACCURACY AND TOLERANCES OF POWDER BED BASED AND NOZZLE BASED ADDITIVE MANUFACTURING PROCESSES

 # LAM 301

Samira Gruber[1,3], Christian Grunert[1], Mirko Riede[1], Elena López[1], Axel Marquardt[3], Frank Brueckner[1,2], Christoph Leyens[1,3]

[1] Fraunhofer Institute for Material and Beam Technology, IWS, Winterbergstraße 28, Dresden, Germany
[2] Luleå University of Technology, 971 87 Luleå, Sweden
[3] Technische Universität Dresden, Institute of Materials Science, Helmholtzstr. 7, 01069 Dresden, Germany

Keywords: Additive Manufacturing, dimensional accuracy, benchmark artefact, Laser Metal Deposition, Laser Powder Bed Fusion, Electron Beam Melting

Abstract

Additive Manufacturing (AM) processes have the potential to produce near-net shaped complex final parts in various industries such as aerospace, medicine or automotive. Powder bed based and nozzle based processes like Laser Metal Deposition (LMD), Laser Powder Bed Fusion (LPBF) and Electron Beam Melting (EBM) are commercially available, but selecting the most suitable process for a specific application remains difficult and mainly depends on the individual know-how within in a certain company. Factors such as the material used, part dimension, geometrical features as well as tolerance requirements contribute to the overall manufacturing costs which need to be economically reasonable compared to conventional processes.

Within this contribution the quantitative analysis of basic geometrical features such as cylinders, thin walls, holes and cooling channels of a special designed benchmark demonstrator manufactured by LMD; LPBF and EBM is presented to compare the geometrical accuracy within and between these processes to verify existing guidelines, connect the part quality to the process parameters and demonstrate process-specific limitations.

The fabricated specimens are investigated in a comprehensive manner with 3D laser scanning and CT scanning with regard to dimensional and geometrical accuracy of outer and inner features. The obtained results will be discussed and achievable as-built tolerances for assessed demonstrator parts will be classified according to general tolerance classes described in [1, 2].

Introduction

Even though the geometrical complexity obtained by AM is seen as the main advantage compared to conventional processes, AM inherent geometrical limitations still exist and are partly addressed in design guidelines [3–8]. These guidelines were mostly developed for LPBF using a specific machine and material. The first benchmark artefacts for AM were designed in 1991 by Kruth [9] for stereolithography and since then, more than 60 geometrical benchmarks have been designed to evaluate dimensional or geometrical accuracy, repeatability and minimum feature size [10] of AM parts. These existing benchmarks either concentrate on only a few features or are very complex and hard to measure accurately due to features being too close together. Therefore, the aim of this study was to design, build and test a scalable demonstrator to quantify the geometrical limitations of different powder based metal AM processes.

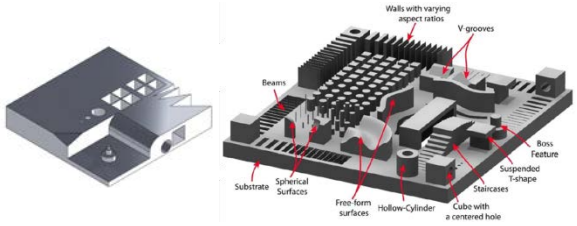

Figure 1: First simple LPBF benchmark [11] (left), benchmark design with high complexity [12] [10] (right)

The new design developed at Fraunhofer IWS was already used for comparison of EBM demonstrators and LPBF demonstrators in [13]. But the analysis was mainly focused on average deviations, not looking further into the relationship between feature size and achievable accuracy, which is addressed here.

Furthermore, an LMD demonstrator is included in the analysis.

The methodology to investigate the geometrical capability of certain additive manufacturing processes in terms of dimensional accuracy and tolerances is divided into the following four steps:

1. Design of a benchmark artefact incorporating geometric characteristics referenced in [14]
2. Manufacture benchmark artefacts using three different AM processes LPBF, EBM and LMD
3. Measure geometrical features according to defined test plan with 3D scanning and CT scanning and
4. Analyze results and compare manufacturing processes and measuring techniques with regard to the general tolerance capability.

Demonstrator Design

A new benchmark demonstrator (see Figure 2) with the base dimensions 40x40x15 mm³ was designed according to the following specifications:

- different geometrical elements (cylinder, prism, sphere, freeform) acc. to [15]
- surfaces facing up and down
- different feature sizes
- internal features (cooling channels or holes) with regard to removing excess powder
- sufficient distance between features for access for 3D scanning
- feasible and scalable for all AM processes
- feature reduction where possible (3-5 feature variations per element) to reduce measurement time and cost.

Overall, the benchmark consists of 64 geometrical elements. For each element, a test plan was created taking into account dimensional and form tolerancing. The test plan is described in detail in Table 3 in the section “Inspection Techniques”.

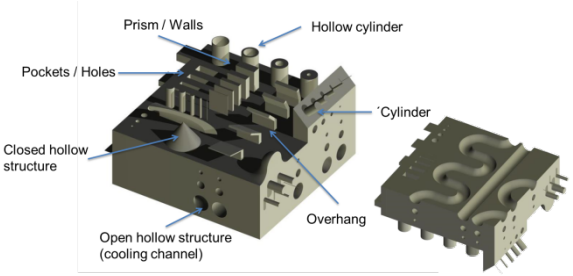

Figure 2: Newly designed benchmark overview (left), cooling channels of different diameter and paths (right)

Manufacturing

Process Equipment

For this investigation, three different metal additive manufacturing processes were chosen: Laser Powder Bed Fusion (LPBF), Electron Beam Melting (EBM) and Laser Metal Deposition (LMD). In this section, the different process principles and manufacturing conditions are shortly described (see Figure 3). LPBF and EBM are powder bed based processes where a single powder layer is spread and selectively molten and fused by a laser/ electron beam which is deflected by a mirror system or electro magnetically. The build plate is then lowered, a new powder layer is spread and the process continues until the part is fully built.

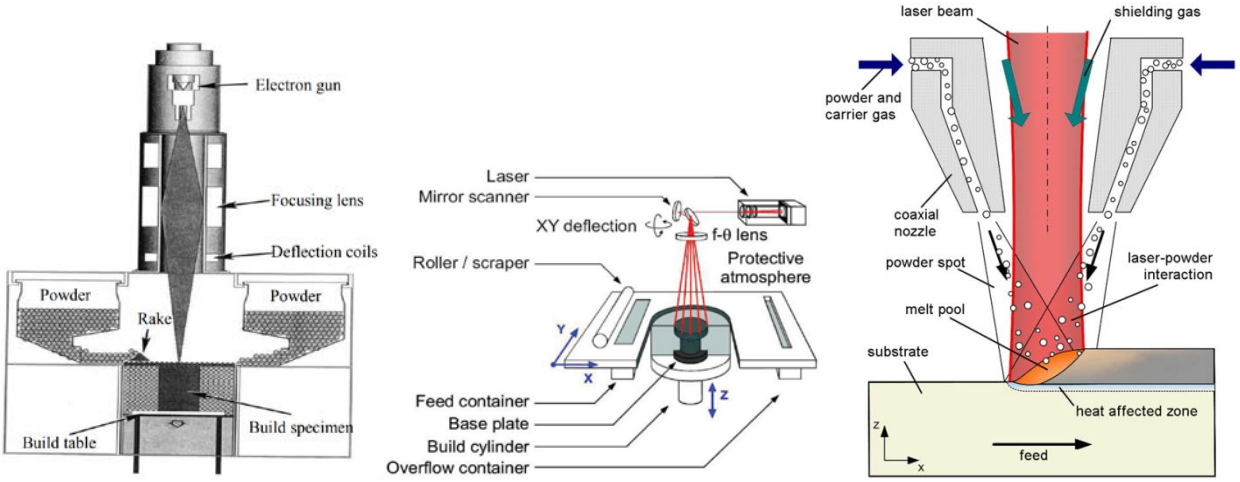

Figure 3: Schematic view of EBM process [16] (left), LPBF process [17] (middle) and LMD process according to [18] (right)

EBM has the advantage of high scanning speeds and preheating of each powder layer prior scanning in a vacuum chamber up to 1100 °C lowering thermally induced stresses and enabling processing of materials with a high ductile-to-brittle transition temperature such as titanium aluminides [19]. LMD is a nozzle based process where powder delivered through a nozzle onto a substrate is preheated and melted when passing a focused laser beam close to the substrate. The main advantage of LPBF and EBM is the high geometrical complexity, whereas LMD allows for near net shaped scalable geometries ranging from µm structures to large components with build rates up to 10 g/min.

Table 1 gives an overview on the process-material-combinations as well as the machine setup and process parameters used specifically for this study. For the two LPBF demonstrators, the original parameter sets provided by the manufacturer were used without optimization, therefore representing "typical" process conditions. For LMD and EBM, the process parameters for the chosen materials were developed in previous trials.

Table 1: Machine setup for LPBF, EBM and LMD

Process	LPBF	LPBF	LMD	EBM
Machine	Renishaw AM250	SLM 250HL	Lasertec 65	Arcam A2x
Material	IN718	Ti-6Al-4V	IN718	Ti-5553
Scan Strategy	Stripes, Border	Chess, Contour + Border	Individual for each feature	Lines, Contour
Energy Source	Laser			Electron Beam
Spot size	75 µm	75 µm	1.7 mm	200 µm
Layer thickness	30 µm	50 µm	200 to 650 µm	70 µm

Powder Material

Two material classes for Additive Manufacturing were chosen: the titanium alloys Ti-6Al-4V for LPBF and a newly developed alloy Ti-5Al-5Mo-5V-3Cr (Ti-5553) for EBM and the nickel-based alloy Inconel 718 (IN718) for LPBF and LMD. This configuration allows the comparison of two materials and one process (LPBF) and one material and two processes (LPBF-EBM, LPBF-LMD). Ti-6Al-4V is the most common used alpha-beta titanium alloy in the aerospace /automotive /dental industry with a density of 4.43 g/cm³ and provides a high specific stiffness. Inconel 718 has a density of 8.19 g/cm³ and is widely used in high temperature applications such as turbomachinery.

As can be seen in Figure 4, all powders show a spherical shape and low amount of agglomerates. The LPBF powders have a particle size distribution of 15-45 µm. The LMD and EBM powder have a particle size distribution of 50-150 µm.

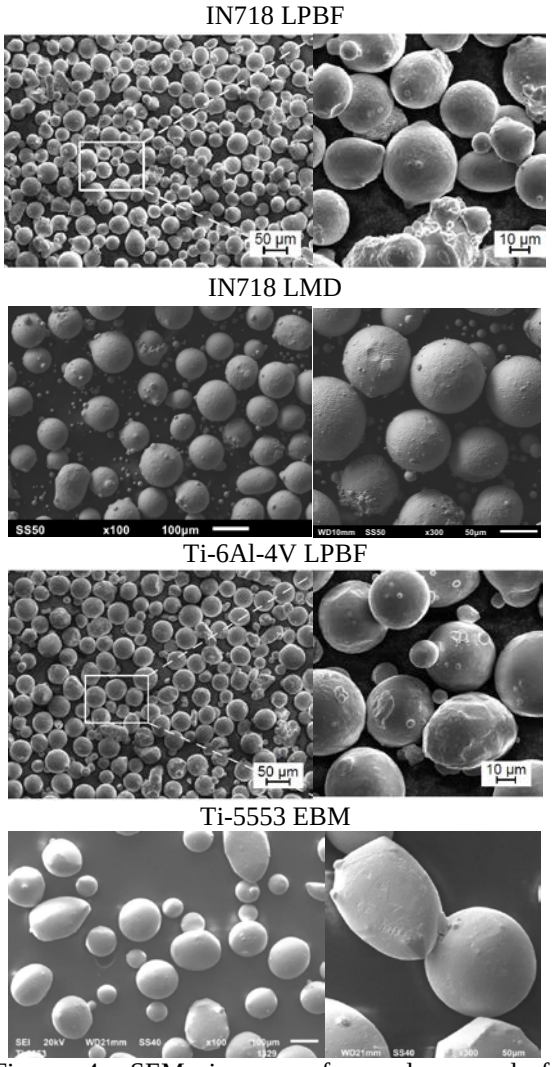

Figure 4: SEM images of powders used for demonstrator manufacturing

Benchmark demonstrator manufacturing

LPBF and EBM

After conversion to a STL-file the part is orientated and positioned in the build chamber using the software Magics from Materialise and then sliced and assigned the process parameters. The scan strategy varies depending on the process and software used. As can be seen in Figure 5, the scan strategy for the Ti-6Al-4V demonstrator in this study consisted of a borderline (red) with an offset to the edge of the STL boundary due to the beam size, two additional borderlines and the hatch to fill the element. Vertical

walls of the smallest thickness were scanned with two straight borderlines.

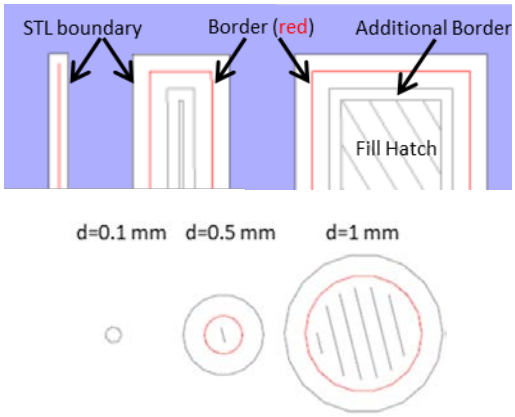

Figure 5: Example of LPBF scan strategy for vertical walls of Ti-6Al-4V demonstrator (top), vertical cylinders (bottom)

It is expected that relative deviations of the width of the smallest wall will therefore be high. Small closed outer contours are neglected by the software and will therefore not be manufactured. That was the case for the smallest vertical cylinder with a diameter of 0.1 mm as can be seen in Figure 5 where no borderline is activated. The cylinder with d=0.5 mm still has a border line and hatch fill line. Consequently, the LPBF process resolution also depends on the software capabilities.

LMD

The process parameters and scan strategy for LMD was determined for each geometrical element individually in an iterative manner. The geometry was scaled by factor 1.7 to ensure accessibility and manufacturability since the laser spot size was 1.7 mm and lower distances between features would have led to collisions with the powder nozzle. The geometry of the cooling channels proved to be challenging when closing the circular shaped channels. Therefore, only the three largest outer cylinders, hollow cylinders and walls were manufactured. For the overhang angle, all 5 overhangs were realized. The scanning strategies for the individual elements are shown in Table 2. The scanning strategy for the base geometry was meander with a double contour to increase dimensional accuracy.

All features were manufactured using three axes. All built demonstrators are depicted in Figure 6. Visual inspection already shows process inherent differences in resolution and size. These demonstrators were thoroughly analyzed as described in the following sections.

Table 2: LMD scanning strategies for single features

Feature	No.	Scanning Strategy
Cylinder	1 2 3	2 circular beads 1 bead + 1 centric pulse 1 pulse All with P = 300 W, pulsed
Thin walled hollow cylinder	1 2 3	2 overlapping circular beads 1 circular bead 1 circular bead All with P = 500 W, pulsed
Vertical/ Horizontal walls	1 2 3	Meander, P = 400 W, pulsed 2 beads, P = 500 W, cw 1 bead, P = 500 W, cw
Overhang	1-5	For all P = 500 W, 1 bead

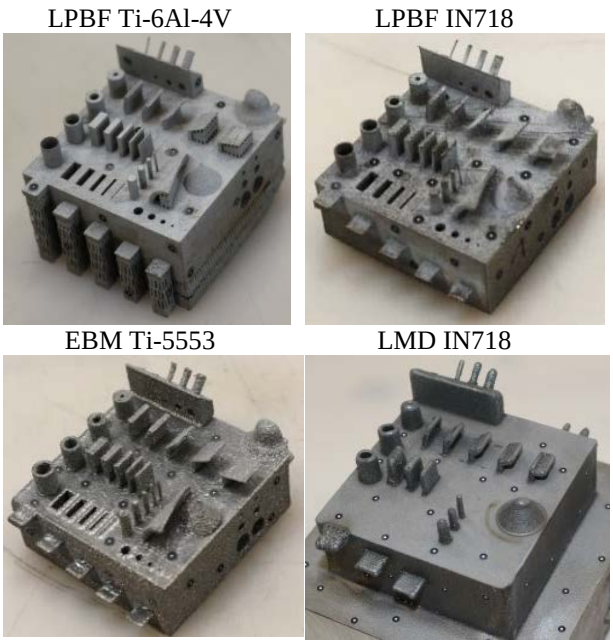

Figure 6: Overview of manufactured demonstrators

Inspection Techniques

Test Plan

The test plan in Table 3 lists all features and corresponding characteristics analyzed in this contribution. Besides linear and angular dimensions [1], form (flatness, cylindricity) [14, 20, 21] orientation (perpendicularity) and location tolerances (position to plane) were investigated. According to [14], the flatness is defined as the smallest distance between two parallel planes enveloping a surface. Cylindricity merges straightness and circularity to describe the conformity to a perfect cylinder. It describes the distance of two concentric cylinders in which all points of the surface of the cylindrical feature fall.

Table 3: Test plan for demonstrators

Description		Dimension	Tolerances		
Element	**Name**		**Form**	**Orientation**	**Location**
base geometry	A, B, C, D, top	length, width, height	flatness	-	-
vertical wall	VW1-5			perpendicularity	position to top surface and side surfaces A,B
horizontal wall	HW1-5				
pocket	P1-5				
overhang	OH1-5	angle		-	
hollow cylinder	HC1-4	diameter, height	cylindricity	perpendicularity	
vertical cylinder	VC1-5				
45° cylinder	C451-5				
horizontal cylinder	HC1-5				
holes	H1-5	diameter			
cooling channel	CC				

Angularity is defined as an angle between an inclined surface and a base surface where the inclined surface lies between two planes with a defined distance. Perpendicularity is angularity at an angle of 90°. Position specifies the deviation from specified dimensions of a feature on a part. For all described tolerances the following applies: the larger the value the larger the deviation from the CAD file

3D Scanning

3D scanning with the GOM ATOS Core 45 (Figure 7) was used for dimensional and form analysis of outer features with a resolution of 5 µm. Two cameras record a fringe pattern projected onto the surface of the part, thus a point cloud of the surface is generated, converted to a polygon mesh and then analyzed using the software Polyworks. When features stand too close together, points of the surface are missing and therefore the accuracy of the measurements is negatively impacted (Figure 8). In this case, the demonstrator was scanned several times in different angles to get better access to critical regions.

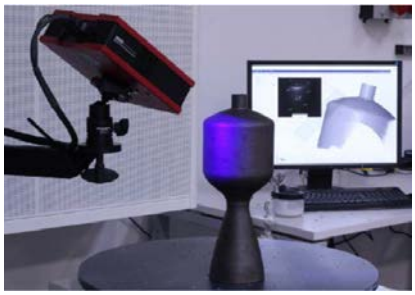

Figure 7: 3D Scanner GOM ATOS Core 45

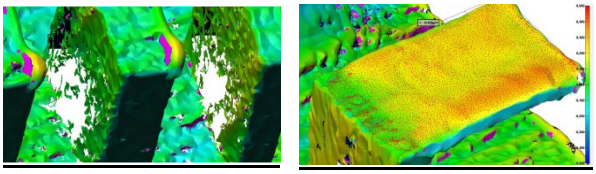

Figure 8: Limitations in 3D scanning, left: missing points, right: approximation of plane

Computed tomography

For the set-up in this investigation, an YXLON FF35 CT equipped with a 250 kV reflection X-ray vacuum tube with minimum spot size of ≤ 6 µm was used. Computed tomography produces cross-sectional (tomographic) images of a scanned object by combining numerous high intensity X-ray measurements taken from different angles. The X-rays attenuate during penetration of the object due to absorption and scattering. From the detected signals an image with different grey values per voxel is reconstructed. The quality of CT scans is problematic at high material density since the penetration depth of X-rays decreases and objects are not properly recognized. Therefore, the large LMD INC718 demonstrator could not be analyzed with the available CT system.

Polyworks

The software “Polyworks” was used to measure dimensions and tolerances from the polygon meshes created with 3D scanning and computed tomography. Auxiliary planes from the surfaces were created using the best-fit method (Figure 9). The graphs were created with the freeware Gnuplot.

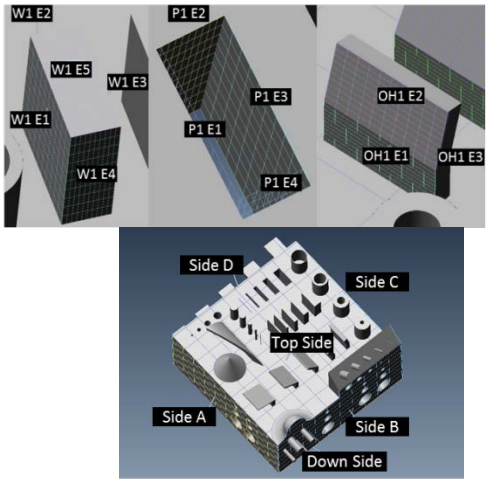

Figure 9: Definition of planes for different features (left: vertical wall, middle: pocket, right: overhang, bottom: base geometry)

Results

Figure 10 gives an overview of the manufactured demonstrators and presents the 3D scan fitted to the top surface and side surfaces A and B of the CAD file. Green marks very low deviation from the CAD (± 150 µm for the LPBF demonstrators and ± 250 µm for EBM and LMD), orange/ red marks areas with positive deviation, blue marks areas with negative deviations and purple is a deviation larger than ± 1.5 mm for EBM/LMD and ± 0.5 mm for LPBF. Visual inspection of these images shows the tendency that smallest features are larger and overall dimensions of the base plate are smaller than the CAD file.

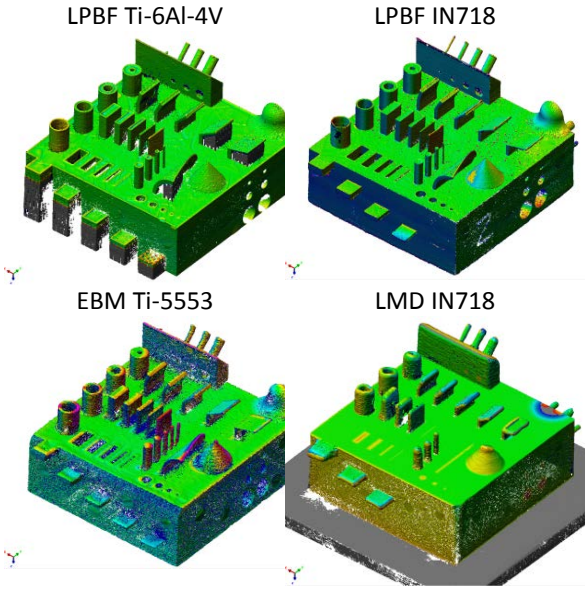

Figure 10: 3D Scan vs. CAD file for all demonstrators, green indicating a deviation within ±150 µm for LBPF and ± 250 µm for EBM and LMD

Besides the smallest diameter of 0.1 mm, all other features were successfully built and could be analyzed according to the test plan (Table 3).

Quality of CT measurements

For the EBM demonstrator, the CT and 3D scan results of the outer features were compared (Figure 11). Overall, the smallest deviations were found for the dimensional values and form tolerances such as flatness and cylindricity, see Table 4. Relative deviations remained large (>20%) given the small absolute values of some tolerances. For example, the perpendicularity of the widest vertical wall (VW1) was measured by 3D scan to be 0.062 mm. The corresponding CT value was 0.079 mm which is a relative deviation of 27 %.

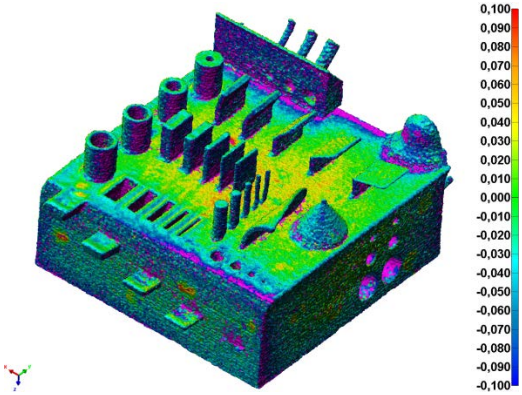

Figure 11: CT vs. 3D scan of EBM Ti-5553

Table 4: Absolute average deviations of CT and 3D scan results for EBM Ti-5553 demonstrator

in mm	Dimension	Form	Perpen-dicularity	Position
Average	0.074	0.028	0.084	0.1235

Overall, the CT scans and 3D scans follow the same trends and lead to the same conclusions regarding the geometrical accuracy. For outer features, 3D scanning is a faster inspection technique and material-independent compared to CT scanning and therefore advantageous. For inner features, CT scanning presents a non-destructive inspection technique and is especially suited to measure the accuracy of additively manufactured parts with internal complex structures. From the CT scans in Figure 12 it is clearly visible that the pockets and meander cooling channels of the EBM demonstrator are sealed with sintered powder that could not be removed after the build process. Additionally, the pockets demonstrate an increasing shift in the upper region to the right generated during the build process. It is unclear, why this shift occurred during the build process but it

could be attributed to the rake mechanism and different cooling rates of the part after finishing the base geometry. Similar EBM build defects were investigated in [22] classified as loss of edge due to different cooling rates at free ends of the part. In contrast, the LPBF IN718 demonstrator presents straight pockets with no remaining powder.

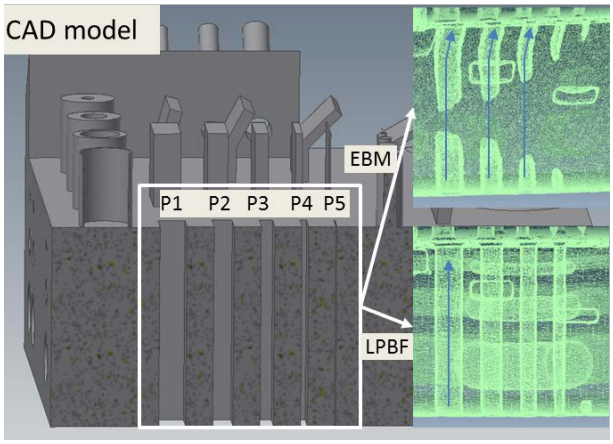

Figure 12: CAD model compared to CT scans of pockets - EBM Ti-5553 with sintered powder and constant shift and LPBF IN718 with straight pockets)

Dimensional Results

The measured linear dimensions length (base dimension), width (prisms), diameter (cylinder) and angular dimension (overhang angle) were compared to the CAD file and the resulting relative deviations are presented in Figure 13. For the base geometry, all processes show low deviations below 5 %. The dimensional deviations for the smallest vertical walls rose to more than 300 % for LPBF and EBM. The smallest achievable wall thickness was 303 µm. In the literature, it has been shown that an optimization of process parameters can lead to smaller wall thicknesses of 140 µm [23] but this was not the target of this study. The LPBF Ti-6Al-4V demonstrator is consistently more accurate by factor 10 than the LPBF IN718 demonstrator. This proves that the choice of process parameters and materials can lead to significant differing dimensional accuracy within the same process. For vertical walls, the LMD deviations were in the range of the EBM deviations and more accurate than the IN718 LPBF demonstrator. The accuracy of all overhang angles was below 5 % for the LPBF and EBM processes. The LMD process had large deviations above 10 % for overhang angles below 60°. This deviation may be improved with further optimization of process parameters. For the diameters of cylinders and holes the dimensional accuracy also increased with smaller diameters similar to the findings of walls and pockets. The orientation of cylinders had no impact on the accuracy for all processes. The largest differences in the accuracy of the LPBF demonstrators was found for the inner features pockets and holes.

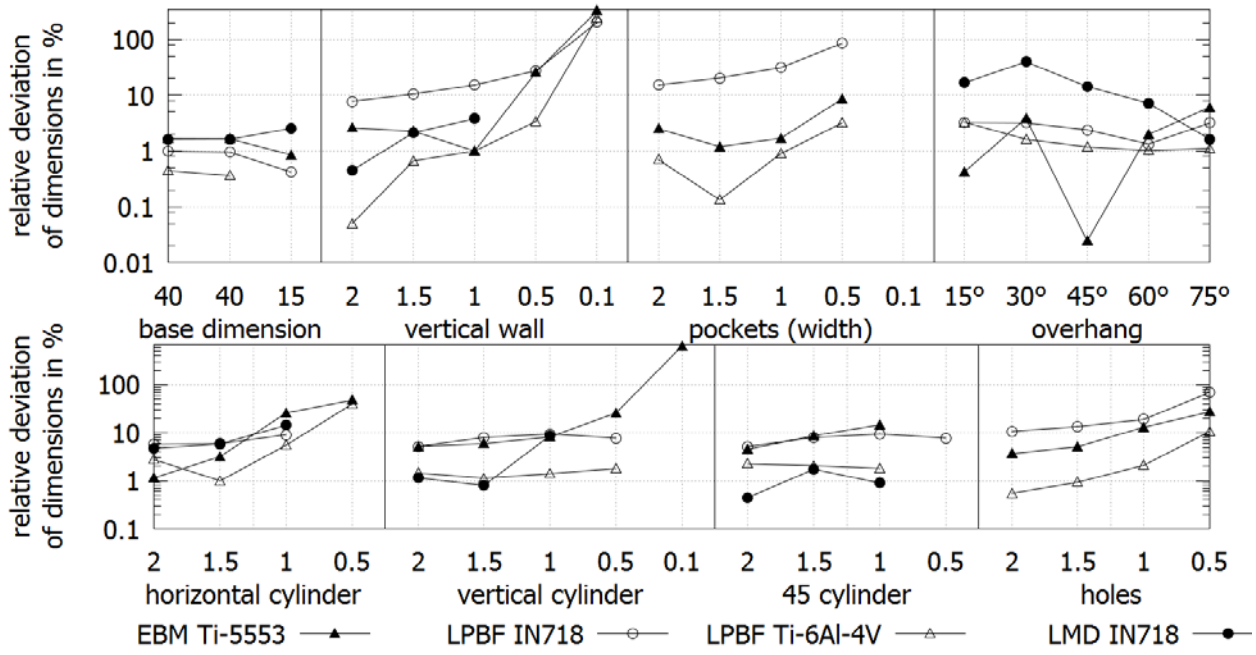

Figure 13: Comparison of relative dimensional deviations for selected features (width for prisms, angle for overhang and diameter for cylinder)

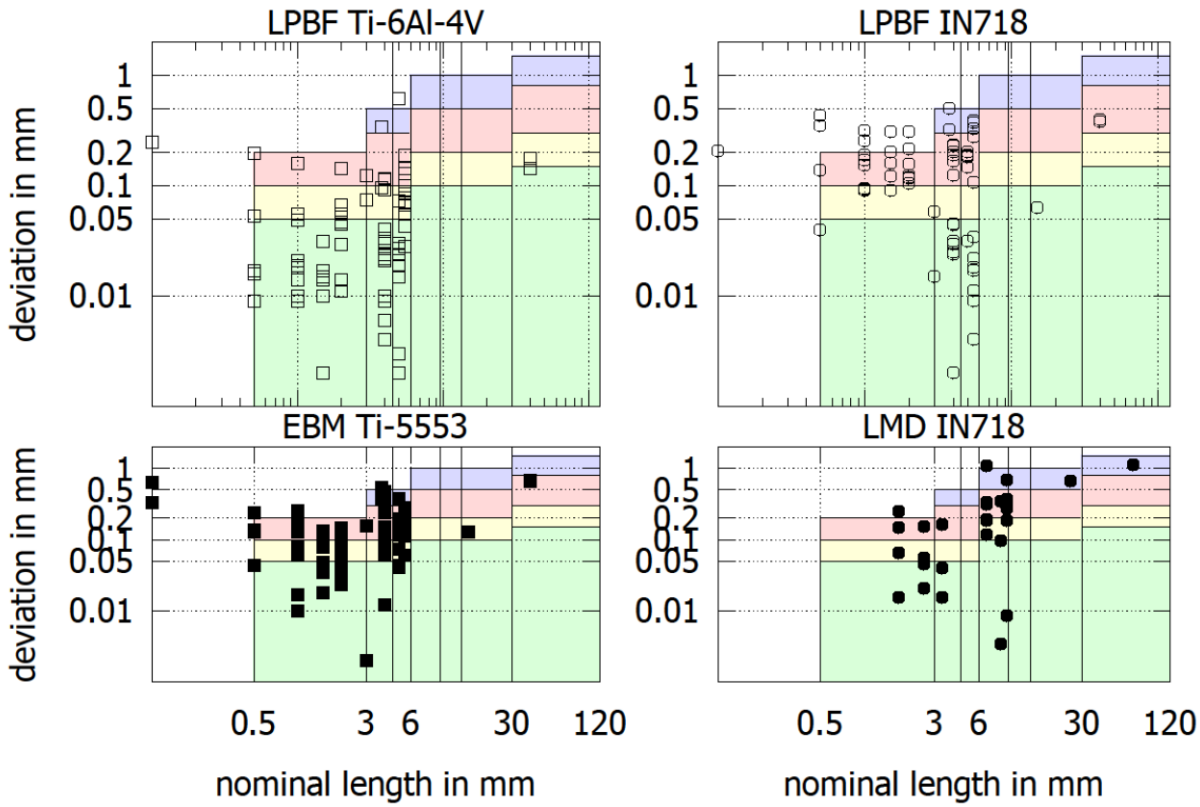

Figure 14: Process-specific absolute deviations of linear dimensions sorted by nominal length and classified into tolerance class (green: fine, yellow: medium, red: coarse, violet: very coarse) acc. to [4]

In Figure 14, all measured absolute linear dimensional deviations are sorted by nominal length and classified by tolerance classes according to [1]. For nominal lengths below 6 mm the majority of dimensional deviations of the LPBF Ti-6Al-4V demonstrator are in the 'fine' tolerance class. The IN718 LPBF demonstrator had larger deviations in the class 'medium' and 'coarse' for nominal lengths between 0.5 and 3 mm. The accuracy of EBM and LMD is comparable and mostly found in class 'coarse'. This is mainly contributed to the higher powder particle size, focus diameter and layer height compared to LPBF (see Table 1).

In summary, the smallest achievable structure size for LPBF is around 300 mm, for EBM 500 µm and for LMD with the tested nozzle 1.2 mm, which was expected due to the different particle sizes and layer thickness of the processes. Smaller structures are possible with LMD when the laser spot diameter, the powder nozzle and powder particle size is adjusted.

Form Tolerance Results

The form tolerances for flatness and cylindricity are presented in Figure 15. The flatness values of the parallel planes E1 and E3 (see Figure 9) representing the long vertical sides were averaged for the base geometry, vertical and horizontal walls, pockets and overhangs. The LPBF process shows lower form and cylindricity values throughout all feature elements and sizes than the EBM and LMD process. The form tolerances for the two LPBF demonstrators are very similar opposed to the high dimensional results (Figure 13). Best overall flatness results were achieved for vertical walls. There was no large dependency of flatness on feature size except for the overhang angle and the smallest vertical wall. The flatness increased consistently with the overhang angle for the LPBF process. This could be explained by increased waviness at high overhang angles due to decreased overhang thickness and resulting remelting of up skin surfaces and borderlines. The high flatness of the smallest vertical wall is also caused by borderline remelting and resulting in a wavy surface. The EBM demonstrator had the largest flatness values for all geometrical features except for the overhang structures where LMD values are larger. Especially the base geometry and pockets have high maximum flatness values caused by the high distortion of the EBM demonstrator on the top surface, which was already anticipated through the CT scan in Figure 12.

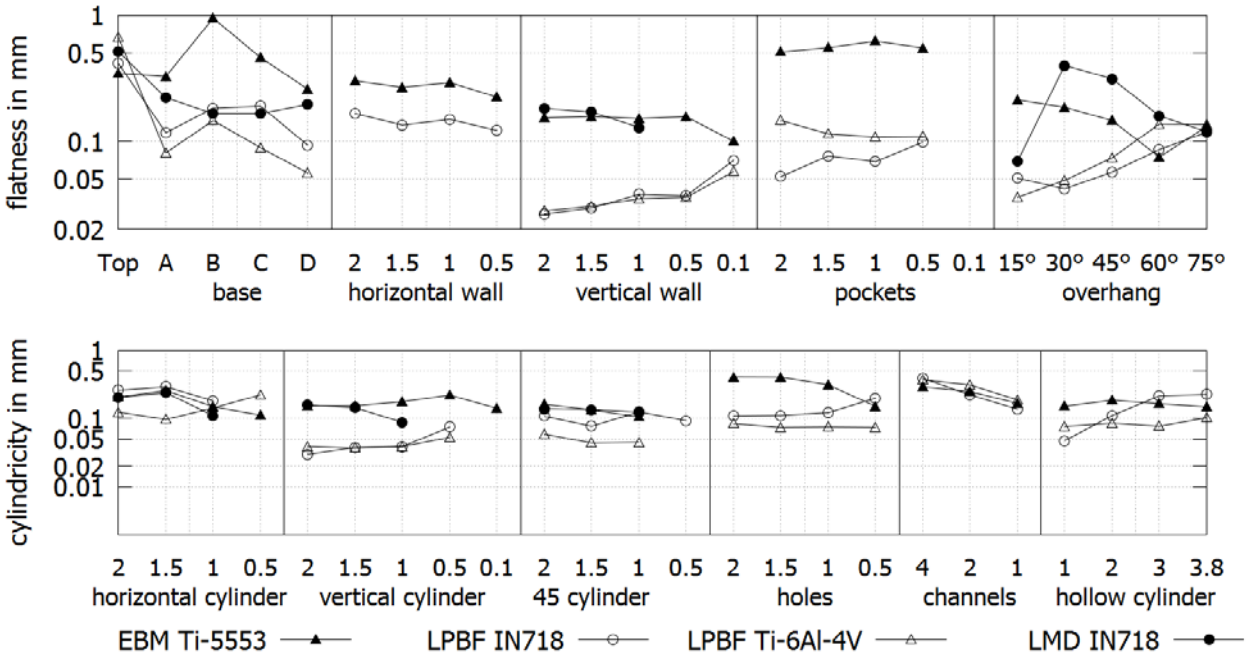

Figure 15: Flatness and cylindricity for selected features for all processes

No significant difference between cylindricity of outer or inner features nor a feature size dependency was found for all processes. All processes show similar results leading to the conclusion that cylindric elements are well suited for the layer-wise Additive Manufacturing processes. When summarizing all flatness values and sorting them by nominal length, it can be seen in Figure 16 that the LPBF processes were not able to reach the 'fine' tolerance class for features smaller than 10 mm. Instead, the flatness ranges evenly between tolerance classes 'medium' and 'coarse'. For the LMD and EBM process the flatness values are hardly in the 'coarse' tolerance class and mostly even exceed the specified tolerance classes. This leads to the conclusion that the EBM and LMD process still need machining as a post process to meet tolerance specifications whereas for the LPBF process general tolerances can be met.

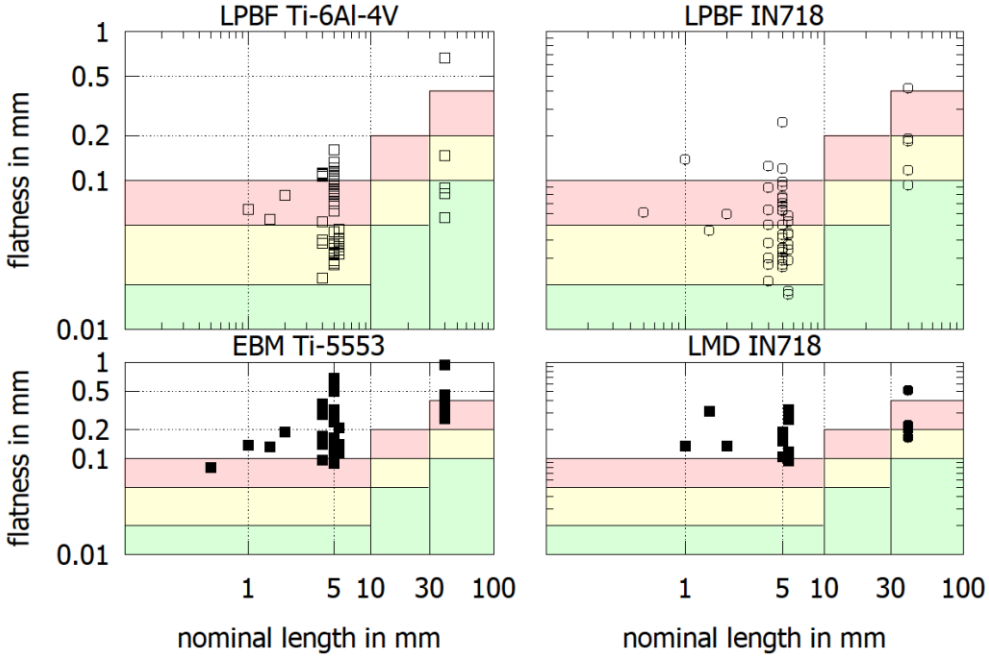

Figure 16: Process-specific flatness vs. nominal length, classified by tolerance class (green: H, yellow: K, red: L) acc. to [5]

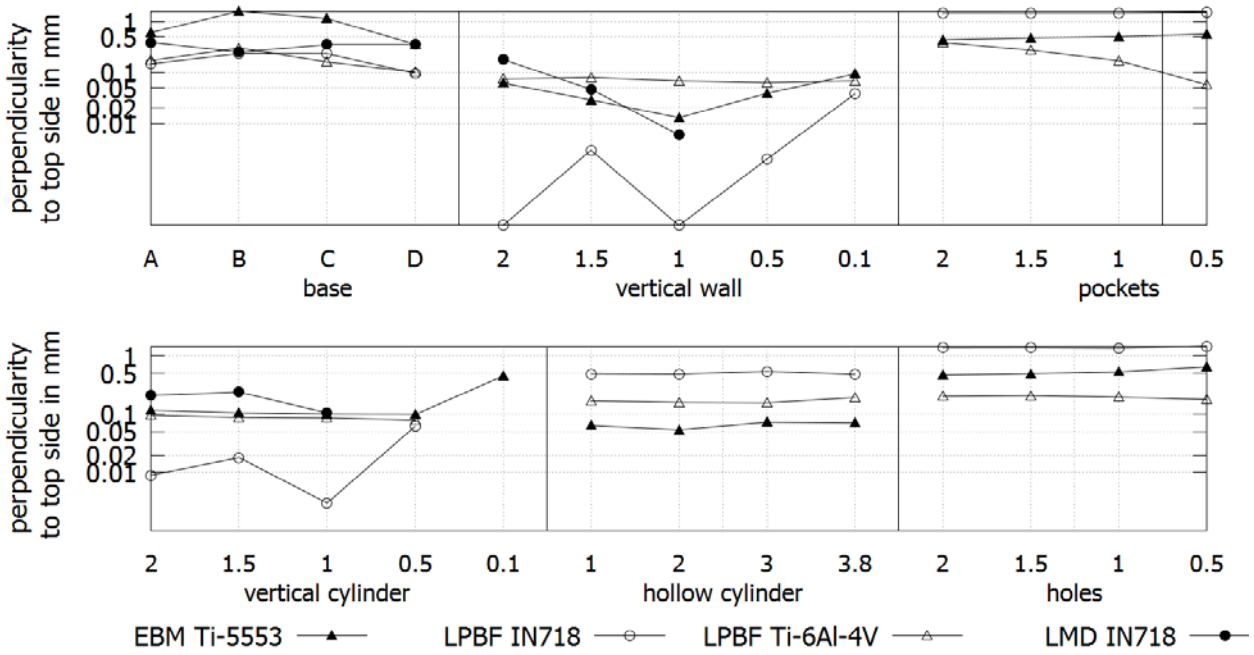

Figure 17: Deviation to perfect perpendicularity of selected features for all processes

The perpendicularity of walls and cylinders to the top base surface is depicted in Figure 17. For features smaller than 100 mm, the classification in [5] lists the following: 'H' for 0.2, 'K' for 0.4 and 'L' for 0.6 mm. For the base geometry, the EBM process showed highest values between 0.5-2 mm and is therefore mostly in class L and above. The results for the vertical walls and vertical cylinders were below 0.1 mm for all processes (except the LMD process for higher feature size) and therefore in class 'H'. The perpendicularity of internal features such as pockets and holes was particularly high (above 1 mm) for the LPBF IN718 demonstrator well exceeding values of the EBM and other LPBF process.

At last, the position to side A for prisms and to side A and B for cylinders was analyzed (see Figure 18). For vertical walls and overhangs, the best position tolerances with values around 0.1 mm were achieved by the Ti-6Al-4V LPBF demonstrator followed by the IN718 LPBF (around 0.3 mm), LMD (around 1 mm) and finally EBM demonstrator (over 2 mm). The large position offset of the EBM demonstrator is caused by the aforementioned shift during build-up (see Figure 12). For the vertical cylinder and hollow cylinder the position tolerance for the two LPBF demonstrators was around 0.3 mm and 0.5 mm opposed to around 2 mm for the EBM and LMD demonstrator.

For inner features such as pockets and holes, the position tolerances of the EBM demonstrator were significantly lower than for corresponding outer features. The IN718 LPBF demonstrator had the opposite effect, inner features had higher position tolerance than outer features.

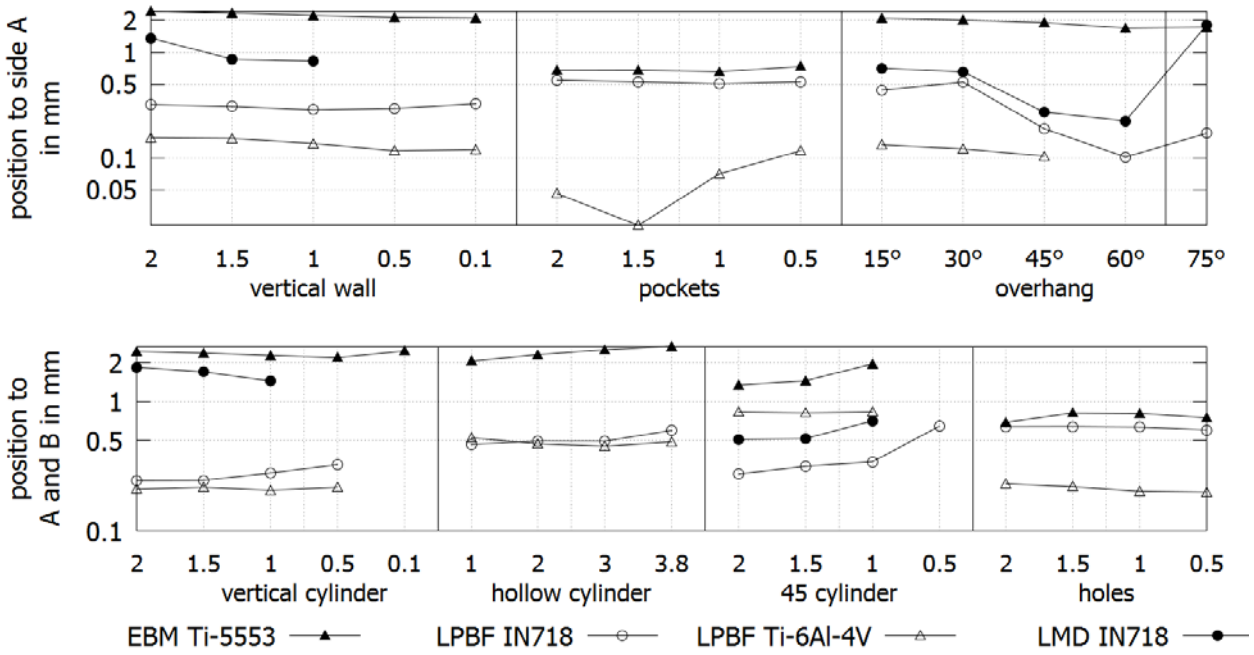

Figure 18: Position tolerance of selected features for all processes

Conclusion

In this study, 3D and CT scanning was used to analyze the geometrical accuracy and tolerances of a special designed demonstrator part. Not only dimensional tolerancing but also form deviations such as flatness and cylindricity as well as perpendicularity and position tolerances were considered. This is important since the end user has certain specifications for the final part and needs knowledge on the geometrical capabilities of different AM processes. The comparison of outer feature results obtained by 3D scanning and CT scanning showed high consistency in the range of ± 100 µm and therefore both techniques are suited to determine the part quality. For inner structures, CT scanning is advantageous compared to 3D scanning.

It was found that the dimensional accuracy highly varies within one demonstrator and therefore not only depends on the process but also on the feature element and size. For example, within the LPBF demonstrator deviations can range between 0.01 and 0.2 mm for the same element size. The following tolerance classes for linear dimensions were reached:

- LPBF: mainly f (fine) for features 0.5-6 mm,
- EBM: mainly m (medium) and c (coarse)
- LMD: large range of deviations, all tolerance classes possible

There were significant differences of the dimensional accuracy between the two LPBF demonstrators leading to the conclusion that the parameter set developed for Ti-6Al-4V was much more accurate. The difference between LPBF and EBM/LMD is mainly attributed to the optimized parameter set and the smaller powder particle size, laser beam spot diameter and layer thickness. Inner structures were best represented by LPBF. The EBM process had sintered powder remnants in the cooling channels and the channel geometry was extremely challenging for the LMD process.

Form deviations such as flatness and cylindricity were lowest for the LPBF process but the tolerance class ‘H’ was not reached. EBM and LMD values were mostly higher than tolerance class ‘L’. The results for perpendicularity and position were similar and showed clearly the advantage of the LPBF process.

Overall, the LPBF provides highest accuracy for dimensions, as well as form, perpendicularity and position tolerance. The EBM / LMD process for now is not suitable for complex internal structures due to sintered powder in the case of EBM and complex programming in the case of LMD. The results are partially attributed to the difference in powder particle size and difference in spot size used for the different processes. LMD accuracy is comparable to the EBM process but still has high potential for increased accuracy at high build-up rates in the future through optimized process parameters and automated tool path generation. In future studies, the effect of the powder particle size on the roughness quality could be investigated as well as how much dimensional

accuracy and tolerancing could be improved by adjusting and optimizing the process parameters. The results of this study underline the need for mechanical reworking of functional surfaces of AM parts to meet specifications and tolerances as well as the need to further improve process parameter development.

References

[1] DIN ISO 2768-1. 1991. *Allgemeintoleranzen - Teil 1: Toleranzen für Längen- und Winkelmaße ohne einzelne Toleranzeintragung*. Accessed 26 February 2018.

[2] DIN ISO 2768-2. 1991. *Allgemeintoleranzen - Teil 2: Toleranzen für Form und Lage ohne einzelne Toleranzeintragung*. Accessed 26 February 2018.

[3] Adam, Guido A. O. 2015. *Systematische Erarbeitung von Konstruktionsregeln für die additiven Fertigungsverfahren Lasersintern, Laserschmelzen und Fused Deposition Modeling*. Forschungsberichte des Direct Manufacturing Research Centers 1. Shaker, Aachen.

[4] Kannan, T. R. 2017. *Design for Additive Manufacturing*. https://www.assemblymag.com/articles/93741-design-for-additive-manufacturing. Accessed 3 January 2018.

[5] Kranz, J., Herzog, D., and Emmelmann, C. 2015. Design guidelines for laser additive manufacturing of lightweight structures in TiAl6V4. *Journal of Laser Applications* 27, S1, S14001.

[6] Mani, M., Lee, J., and Witherell, P. 2017. Design Rules for Additive Manufacturing: a Categorization. In *ASME 2017 International Design Engineering Technical Conferences and Computers and Information in Engineering Conference*. *August 6-9, 2017, Cleveland, Ohio, USA*. American Society of Mechanical Engineers, New York, N.Y., V001T02A035. DOI=10.1115/DETC2017-68446.

[7] Thomas, D. 2009. *The Development of Design Rules for Selective Laser Melting*. Ph. D. Thesis, University of Wales Institute.

[8] Thompson, M. K., Moroni, G., Vaneker, T., Fadel, G., Campbell, R. I., Gibson, I., Bernard, A., Schulz, J., Graf, P., Ahuja, B., and Martina, F. 2016. Design for Additive Manufacturing. Trends, opportunities, considerations, and constraints. *CIRP Annals* 65, 2, 737–760.

[9] Kruth, J. P. 1991. Material Incress Manufacturing by Rapid Prototyping Techniques. *CIRP Annals - Manufacturing Technology* 40, 2, 603–614.

[10] Rebaioli, L. and Fassi, I. 2017. A review on benchmark artifacts for evaluating the geometrical performance of additive manufacturing processes. *The International Journal of Advanced Manufacturing Technology*, 93, 2571–2598.

[11] Kruth, J. P., Vandenbroucke, B., van Vaerenbergh, J., and Mercelis, P. 2005. Benchmarking of different SLS/SLM processes as Rapid Manufacturing techniques. In *International Conference Polymers & Moulds Innovations (PMI)*.

[12] Hao, B., Korkmaz, E., Bediz, B., and Ozdoganlar, O. B. 2014. A novel test artefact for performance evaluation of additive manufacturing processes. In *Proceedings of dimensional accuracy and surface finish in additive manufacturing*. *ASPE spring topical meeting ; April 13 - 16, 2014, University of California - Berkeley, Berkeley, California, USA*. ASPE, Raleigh, NC, Raleigh, NC, 167–172.

[13] Lopez, E., Felgueiras, T., Grunert, C., Brückner, F., Riede, M., Seidel, A., Marquardt, A., Leyens, C., and Beyer, E. 2018. Evaluation of 3D-printed parts by means of high-performance computer tomography. *Journal of Laser Applications* 30, 3, 32307.

[14] DIN EN ISO 1101. 2006. *Geometrische Produktspezifikation (GPS) – Geometrische Tolerierung – Tolerierung von Form, Richtung, Ort und Lauf*.

[15] Gröger, S. 2013. *Funktionsgerechte Spezifikation geometrischer Eigenschaften mit dem System der Geometrischen Produktspezifikation und -verifikation*. Habilitation, TU Chemnitz.

[16] Gong, H., Rafi, K., Starr, T., and Stucker, B. 2013. The Effects of Processing Parameters on Defect Regularity in Ti-6Al-4V Parts Fabricated By Selective Laser Melting and Electron Beam Melting. In *24th Annual International Solid Freeform Fabrication Symposium - An Additive Manufacturing Conference*, 424–439.

[17] Müller, M., Riede, M., Eberle, S., Reutlinger, A., Brandão, A. D., Pambaguian, L., Seidel, A., López, E., Brueckner, F., Beyer, E., and Leyens, C. 2018. Microstructural, mechanical and thermo-physical characterization of hypereutectic AlSi40 fabricated by Selective Laser Melting. In *37th International Congress on Applications of Lasers & Electro-Optics (ICALEO)*.

[18] Brückner, Frank. 2012. *Modellrechnungen zum Einfluss der Prozessführung beim induktiv unterstützten Laser-Pulver-Auftragschweißen auf die Entstehung von thermischen*

Spannungen, Rissen und Verzug. Zugl.: Dresden, Techn. Univ., 2011. Fraunhofer Verl., Stuttgart.

[19] Seidel, A., Davids, A., Polenz, S., Straubel, A., Maiwald, T., Moritz, J., Schneider, J., Marquardt, A., Saha, S., Riede, M., Lopez, E., Brueckner, F., and Leyens, C. 2019. Surface modification of additively manufactured gamma titanium aluminide hardware. *Journal of Laser Applications* 31, 2, 22517.

[20] DIN EN ISO 12781-1. 2011. *Geometrische Produktspezifikation (GPS) – Ebenheit – Teil 1: Begriffe und Kenngrößen der Ebenheit*.

[21] DIN EN ISO 12781-2. 2011. *Geometrische Produktspezifikation (GPS) – Ebenheit – Teil 2: Spezifikationsoperatoren*.

[22] Vo, T. H., Museau, M., Vignat, F., Villeneuve, F., Ledoux, Y., and Ballu, A. 2018. Typology of geometrical defects in Electron Beam Melting. *Procedia CIRP* 75, 92–97.

[23] Yadroitsev, I., Shishkovsky, I., Bertrand, P., and Smurov, I. 2009. Manufacturing of fine-structured 3D porous filter elements by selective laser melting. *Applied Surface Science* 255, 10, 5523–5527.

Samira Gruber studied mechanical and process engineering at the Technical University Darmstadt. In November 2015 she finished her master's thesis about producing defined porous structures with Laser Powder Bed Fusion. Her work at the Fraunhofer IWS focuses on improving the geometrical accuracy of additive manufactured parts.

Christian Grunert completed an apprenticeship as a mechatronic technician at Koenig & Bauer AG in 2011 and is working in the group of 3D Manufacturing at the Additive Manufacturing Center Dresden (AMCD). His tasks include maintenance, servicing and project-specific modifications of machines and equipment. He is involved in several projects, in particular dealing with optical 3D-measurement systems.

Mirko Riede studied mechatronics at the Technische Universität Dresden. In 2011 he finished his master thesis about high precision laser cladding at the Fraunhofer IWS Dresden. For the last 5 years he has been working on several research projects related to additive manufacturing and structuring. Today he is the group manager of 3D Manufacturing at the Additive Manufacturing Center Dresden (AMCD) at Fraunhofer IWS.

Dr. Elena Lopez studied chemical engineering at the Universidad de Valladolid and Friedrich-Alexander-Universität Erlangen-Nuernberg. She finished her PhD thesis about the topic of plasmachemical etching of silicon solar wafers at the Technische Universität Dresden. After focusing on CVD technologies, shemoved to Printing and Additive Manufacturing technologies in 2014. She is the department manager of Additive Manufacturing and Printing at the Additive Manufacturing Center Dresden (AMCD) at Fraunhofer IWS. Nowadays she leads a big consortium named Agent-3D with more than 120 companies involved.

Prof. Dr. Frank Brueckner studied automation and control engineering as well as business administration at the Technische Universität Dresden. He finished his PhD about theoretical aspects of laser cladding. Now he leads the business unit of Additive Manufacturing and Printing at the Fraunhofer IWS Dresden. Together with his team working at the Additive Manufacturing Center Dresden AMCD, he mainly focuses on nozzlebased, powder-bed based processes as well as printing technologies. In addition, he supervises PhD candidates at the Luleå University of Technology.

Prof. Dr. Christoph Leyens studied physical metallurgy and materials technology at RWTH Aachen, Germany, where he earned his diploma in 1993 and his Ph.D. in 1997. He is currently a full professor for materials science and engineering at the Technische Universität Dresden, Germany, and director of the Fraunhofer Institute for Material and Beam Technology, Dresden. Dr. Leyens has covered a wide range of research topics with a focus on high temperature and lightweight materials, surface technology and additive manufacturing. He has published more than 200 papers, seven books and holds eleven patents.